Crystal Structures of Thrombin with Thiazole-Containing Inhibitors: Probes of the S1′ Binding Site

John H. Matthews,* R. Krishnan,* Michael J. Costanzo,# Bruce E. Maryanoff,# and A. Tulinsky*
*Department of Chemistry, Michigan State University, East Lansing, Michigan 48824, and #The R. W. Johnson Pharmaceutical Research Institute, Spring House, Pennsylvania 19477 USA

ABSTRACT Structures of the blood clotting enzyme thrombin complexed with hirugen and two active site inhibitors, RWJ-50353 10080(*N*-methyl-D-phenylalanyl-*N*-[5-[(aminoiminomethyl)amino]-1-[[(2-benzothiazolyl)carbonyl]butyl]-L-prolinamide trifluoroacetate hydrate) and RWJ-50215 (*N*-[4-(aminoiminomethyl)amino-1-[2-(thiazol-2-ylcarbonylethyl)piperidin-1-ylcarbonyl]butyl]-5-(dimethylamino)naphthalenesulfonamide trifluoroacetate hydrate), were determined by x-ray crystallography. The refinements converged at *R* values of 0.158 in the 7.0–2.3-Å range for RWJ-50353 and 0.155 in the 7.0–1.8-Å range for RWJ-50215. Interactions between the protein and the thiazole rings of the two inhibitors provide new valuable information about the S1′ binding site of thrombin. The RWJ-50353 inhibitor consists of an S1′-binding benzothiazole group linked to the D-Phe-Pro-Arg chloromethyl ketone motif. Interactions with the S1–S3 sites are similar to the D-phenylalanyl-prolyl-arginyl chloromethylketone structure. In RWJ-50215, a S1′-binding 2-ketothiazole group was added to the thrombin inhibitor-like framework of dansylarginine *N*-(3-ethyl-1,5-pentanediyl)amide. The geometry at the S1–S3 sites here is also similar to that of the parent compound. The benzothiazole and 2-ketothiazole groups bind in a cavity surrounded by His57, Tyr60A, Trp60D, and Lys60F. This location of the S1′ binding site is consistent with previous structures of thrombin complexes with hirulog-3, CVS-995, and hirutonin-2 and -6. The ring nitrogen of the RWJ-50353 benzothiazole forms a hydrogen bond with His57, and Lys60F reorients because of close contacts. The oxygen and nitrogen of the ketothiazole of RWJ-50215 hydrogen bond with the NZ atom of Lys60F.

INTRODUCTION

The serine protease thrombin plays an important and central role in blood coagulation (Davie et al., 1991). Its most prominent function is the conversion of fibrinogen to fibrin (Blomback et al., 1967; Hogg and Blomback, 1978). Polymerization of the resulting monomers and cross-linking by factor XIII lead to formation of a fibrin network and an insoluble blood clot. Thrombin also activates factor V and factor VIII (Jackson and Nemerson, 1980), and stimulates platelet aggregation and secretion (Hung, et al., 1992). It additionally activates other coagulation proenzymes and is involved in anticoagulation processes by the activation of protein C (Esmon et al., 1982; Esmon, 1989).

A large number of thrombin-inhibitor complexes have been studied by x-ray crystallography (Stubbs and Bode, 1993; Tulinsky and Qiu, 1993; Mathews et al., 1994; Mathews and Tulinsky, 1995; Krishnan et al., 1996). These structures have increased our understanding of the many important roles that thrombin plays and have revealed a wide variety of binding modes and geometries for the enzyme. Most of the inhibitors bind to one or the other of the S1–S3 subsites of the active site and/or the fibrinogen recognition exosite.

Less is known about binding at the S′ sites. The importance of these regions was originally established by binding studies of fibrinopeptide A fragments, which showed that the presence of P3′–P4′ residues lowered K_d by an order of magnitude (Marsh et al., 1983). Binding at S′ subsites of thrombin was first revealed by the structure of the thrombin complex with hirulog 3, a synthetic divalent peptide with both active site and exosite binding moieties that are linked with a pentaglycine spacer to a nonhydrolyzable β-homoarginine at P1 (Qiu et al., 1992). The P1′ glycine occupies a small cavity surrounded by His57, Tyr60A, Trp60D, and Lys60F; forms hydrogen bonds to Lys60FNZ, Ser195OG, and His57NE2 (Fig. 1); and adopts a conformation that would be disallowed for residues with side chains. These observations are in agreement with the preference for smaller residues like glycine and serine at the P1′ position of natural thrombin substrates. Following a bend at the P1′ residue, the remainder of the spacer and most of the C-terminal hirudin-like fragment, hirugen, are in an extended conformation. Binding to the enzyme involving main-chain atoms occurs at the S2′–S4′ subsites. Vacant space in the region of thrombin near these sites suggests that residues with side chains could enhance binding.

Received for publication 12 April 1996 and in final form 5 August 1996.
Address reprint requests to Dr. A. Tulinsky, Department of Chemistry, Michigan State University, East Lansing, MI 48823. Tel.: 517-355-9715, X250; Fax: 517-353-1793; E-mail: tulinsky@cemvax.cem.msu.edu.

Abbreviations used: hirugen, sulfated Tyr63-*N*-acetyl-hirudin 53-64; RWJ-50353, *N*-methyl-D-phenylalanyl-*N*-[5-[(aminoiminomethyl) amino]-1-[[(2-benzothiazolyl)carbonyl[butyl]-L-prolinamide trifluoroacetate hydrate; RWJ-50215, *N*-[4-(aminoiminomethyl)amino-1-[2-(thiazol-2-ylcarbonylethyl) piperidin-1-ylcarbonyl[butyl]-5-(dimethylamino) naphthalenesulfonamide trifluoroacetate hydrate; DAPA, dansylarginine *N*-(3-ethyl-1,5-pentanediyl) amide; NAPAP, *Nα*-(2-napthylsulfonyl-glycyl)-D-*para*-amidino phenylalanylpiperidine. MQPA (argatroban), (2*R*, 4*R*)-4-methyl-1-[*Nα*-(3-methyl-1,2,3,4-tetrahydro-8-quinolinesulfonyl)-L-arginyl]-2-piperidinecarboxylic acid; 4-TAPAP, *Nα*-(4-toluenesulfonyl)-L-*para*-amidino-phenylalanylpiperidine]. PPACK, D-phenyalanyl-prolyl-arginyl chloromethylketone.

0006-3495/96/11/2830/10 $2.00

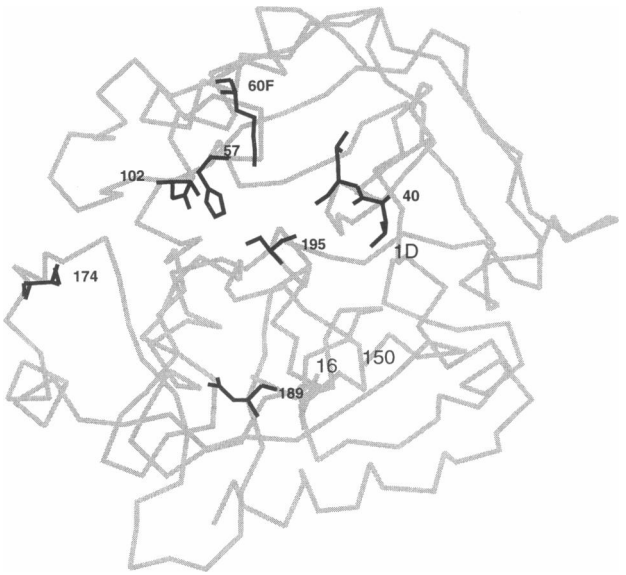

FIGURE 1 Overall view of the C_α structure of thrombin. Pertinent active-site side chain in bold. N-terminals of two chain thrombin are numbered (1D, 16). Gly150 is N-terminal after autolysis loop.

An α-ketoamide group, stable to thrombin cleavage, links the P1 arginine to the pentaglycine spacer in a related class of divalent inhibitors (Krishnan et al., 1996). The x-ray crystal structure of the thrombin complex of one of these molecules, CVS995, shows many of the same S′ interactions. Other comparable divalent inhibitors, called hirutonins, have been developed where cleavage of the scissile bond is prevented by replacing the nitrogen of the amide with a methylene group (DiMaio et al., 1992). In thrombin complexes of hirutonin-2 and hirutonin-6 (Zdanov et al., 1993), molecules with linkers of different length, the inhibitors follow pathways through the S′ binding regions similar to hirulog 3 and CVS995.

We report here the crystallographic results of inhibitors of thrombin with S1′-binding, thiazole-containing groups attached to PPACK and DAPA-like frameworks (Fig. 2) and discuss implications for the future design of inhibitors. The potent inhibitor RWJ-50353 (Fig. 2), with a K_i value of 0.16 nM, resembles the PPACK molecule (Bode et al., 1992), except that the chloromethyl group is replaced with a 2-benzothiazole group. The other molecule, RWJ-50215 (Fig. 2), inhibits thrombin with a K_i value of 1.2 μM and is related to DAPA, an early member of a well-known class of inhibitors based on the chemical nature of thrombin binding sites (Fig. 2) (Okamoto et al., 1976; Hijikata et al., 1976; Nesheim et al., 1979). X-ray crystal structures related to the latter include complexes of human thrombin with NAPAP and argatroban (MQPA, MD-805) at 3.0 Å resolution (Banner and Hadvary, 1991), and bovine ε-thrombin complexed with NAPAP, 4-TAPAP, and argatroban determined at 2.3 Å (Brandstetter et al., 1992). The structures of some of the inhibitor complexes were first determined with trypsin, and the coordinates were used to generate models of binding to thrombin (Bode et al., 1990; Turk et al., 1991). The x-ray structure determination of DAPA complexed with thrombin was similar, showing a binding mode with likenesses to both substrates and hirudin: the P2 dansyl and P1′ piperidine groups of DAPA bind in the S3 and S2 subsites, respectively, whereas the P1 arginine forms an ion pair with Asp189 (Mathews and Tulinsky, 1995).

MATERIALS AND METHODS

Crystallization

The RWJ-50353 and RWJ-50215 inhibitors were synthesized and purified to homogeneity by reverse-phase high-performance liquid chromatography at the R. W. Johnson Pharmaceutical Research Institute (Spring House, PA). Microanalytical data support trifluoroacetate hydrates; percentages of C, H, N and H_2O were within 0.5% of theory. Details of the synthesis and biological activity will be published elsewhere.

Both compounds were used without further purification. An approximately 10-fold molar excess of hirugen was first added to a frozen 1-ml sample of human α-thrombin solution (1.06 mg/ml in 0.75 M NaCl) at 4°C and allowed to thaw to form the complex and prevent autolysis. The ternary complexes were prepared by adding the RWJ inhibitors in 10—15-fold molar excess to the hirugen-thrombin complex. The solutions of the complexes were diluted to 2 ml with 0.1 M phosphate buffer at pH 7.3 and concentrated to about 5 mg/ml by using a Centricon 10 miniconcentrator (MW cutoff 10K) in a refrigerated centrifuge. Crystallization was carried out in 10-μl hanging drops against 1 ml of well solution containing 0.1 M phosphate buffer, pH 7.3, and 27–28% PEG 8000 as previously described (Skrzypczak-Jankun et al., 1991).

Intensity data collection

The RWJ-50353–hirugen–thrombin ternary complex crystal x-ray diffraction data were collected with a Siemens multiwire X-1000 area detector mounted on a Siemens P3/F four-circle goniostat. Graphite monochromated CuKα radiation was generated by a Rigaku RU200 rotating anode source at 7.5-kW power. The crystal-to-detector distance was set at 11.65 cm. The detector swing angle was −15°, the scan range was 0.2°/frame, and each frame was collected for 90 s. The program XENGEN (Howard et al., 1987) was used to process the data to obtain integrated intensities. The crystal diffracted x rays to 2.3-Å resolution with an average peak width of 0.6°.

The RWJ-50215–hirugen–thrombin intensities were measured with an R-AXIS II imaging plate detector and graphite monochromated CuKα radiation from a Rigaku RU200 rotating anode generator, using a fine focus filament (0.3 × 0.3 mm) with a power setting of 5 kW. The crystal-to-detector distance was 75.1 mm, and the crystal diffracted x rays to 1.8-Å resolution. The unit cell dimensions were determined by autoindexing (Higashi, 1990), and the processing of the raw data was carried out with the Rigaku R-AXIS data-processing software package. Both crystals are monoclinic, space group C2, four complexes per unit cell, with a = 70.79 Å, b = 72.53 Å, c = 73.12 Å, β = 101.0° for RWJ-50353, and a = 71.47, b = 72.00, c = 73.39 Å, β = 101.13° for RWJ-50215 (V_m = 2.4 Å^3/Da, protein fraction 51%). The crystals of the RWJ-50353 and RWJ-50215 complexes are isomorphous with hirugen-thrombin and other crystals of binary (Qiu et al., 1992; Krishnan et al., 1996) and ternary complexes (Mathews and Tulinsky, 1995) of thrombin. For the RWJ-50353–thrombin complex, a total of 15,300 independent measurements were obtained from 48,511 collected measurements. Removing weak data with I/sigma(I) < 2 produced a data set of 14,479 unique reflections (75% observed, R_{merge} ($|F|^2$) = 0.054). This data set is complete to 2.5-Å resolution and contains half of the possible reflections between 2.5-Å and 2.3-Å resolution. After the R axis data recorded from RWJ-50215–thrombin were processed, 23,968 independent reflections were obtained from a total of 52,463

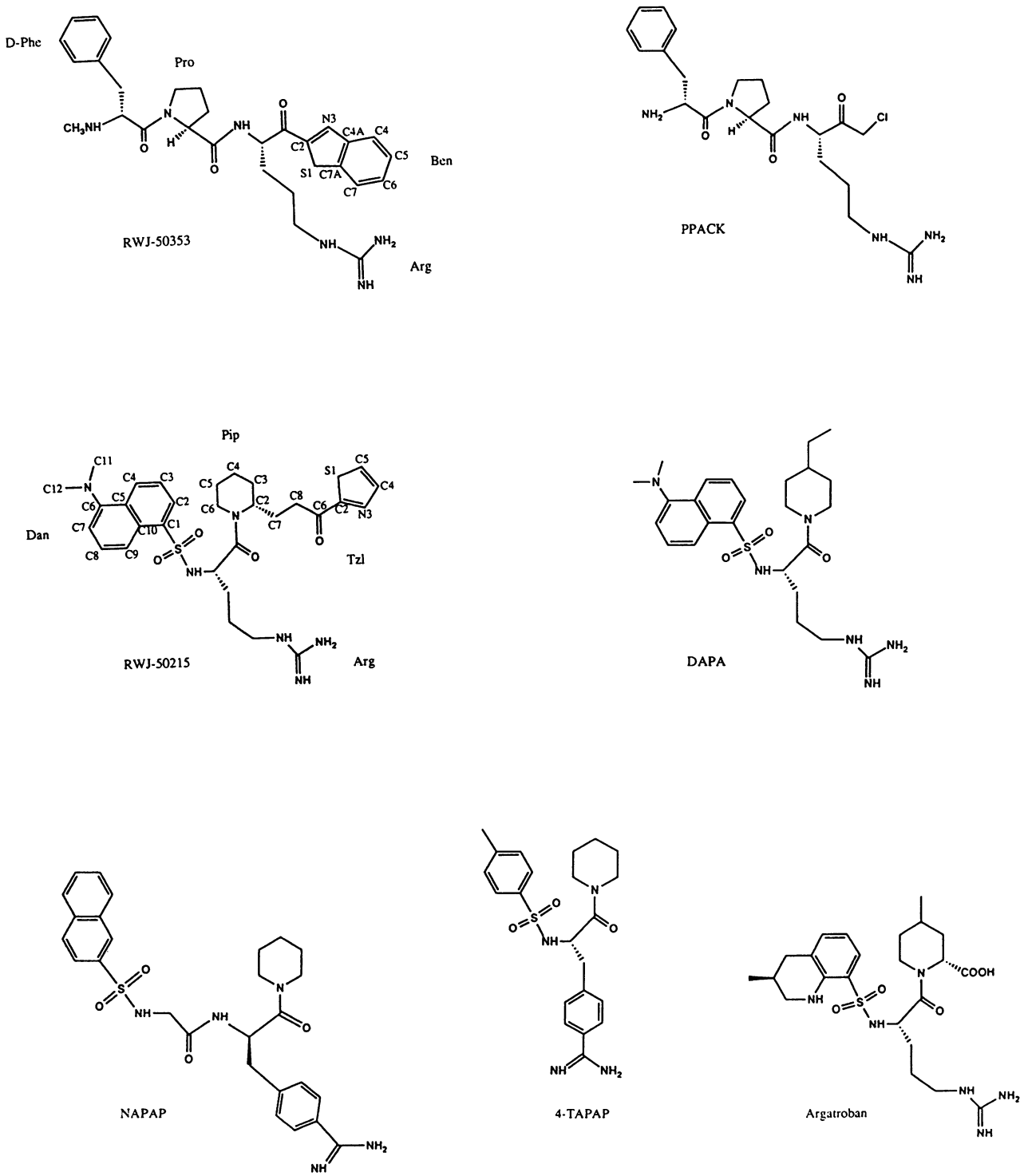

FIGURE 2 Active-site inhibitors of thrombin. RWJ 50353, RWJ 50215 inhibitors in this work. Numbering and nomenclature are as used in text.

observations (20,391 independent reflections after removal of observations with $I < 2$ sigma(I); R_{merge} on $|F|^2 = 0.052$; 80.4% completion at 2.5 Å; 69.5% completion at 1.8 Å).

Structure determination and refinement

The positional and thermal parameters were refined by restrained least-squares methods using the program PROFFT (Hendrickson, 1985; Finzel, 1987). To simplify the dictionary restraints of RWJ-50215, it was treated as four parts (Dan, Arg, Pip, Tzl; Fig. 2).

The phases of the RWJ-50353 and RWJ-50215 complexes were approximated using the thrombin coordinates of the thrombin-hirugen and DAPA-thrombin-hirugen complexes, respectively. The initial crystallographic R-factors were about 0.30 and reduced to 0.20–0.21 after 15–18 cycles of refinement. The first $(2|F_o|-|F_c|)$ electron density maps from 7.0–2.8-Å resolution showed density for most of the thrombin molecule,

with hirugen in the fibrinogen-binding exosite. All of the RWJ-50353 and most of the RWJ-50215 inhibitor were located in the first round of refinement. The linker group between the piperidine and thiazole rings of RWJ-50215 fits the electron density much better when the C2 atom of the piperidine is in the *R*-configuration rather than when *S*-stereochemistry is modeled.

The electron density of the thrombin complexes was compatible with two possible orientations of the benzothiazole (RWJ-50353) and thiazole (RWJ-50215) rings in which the positions of the nitrogen and sulfur atoms are approximately interchanged. The correct position of the sulfur atom of the benzothiazole group was determined by 1) refining in the two possible positions and examining the temperature factors of the sulfur atom, 2) occupancy refinement of the sulfur atom in each position, and 3) examining the possible interactions of the benzothiazole group with thrombin. The first strategy did not produce conclusive results; however, the occupancy refinement clearly established the correct position of the sulfur atom. The occupancy factor of the sulfur (starting at 0.75) increased to 0.86, but decreased to 0.50 in the alternate position. A hydrogen bond (2.7 Å) between the N3 atom of the benzothiazole group and His57NE2 of thrombin further supported the conclusion of the occupancy refinements. The position of the nitrogen atom of a benzoxazole group of a porcine elastase inhibitor makes a similar hydrogen bond with His57NE2 (Edwards et al., 1992).

With RWJ-50215, two independent refinements were carried out on models rotating the thiazole ring approximately 180° with nitrogen atoms at both heteroatom positions. The refinements of both converged with higher occupancy factors for the same nitrogen position. This assignment places the nitrogen in position to form a good hydrogen bond with the NZ atom of Lys 60F (3.0 Å), which is a more chemically reasonable alternative than having the ring sulfur atom make the interaction.

An important structural transition of thrombin has been identified when sodium ion binding to the enzyme induces a conformational change from a slow to a fast kinetic form (Ayala and DiCera, 1994). The physiological sodium ion site was first established crystallographically by rubidium ion exchange (DiCera et al., 1995). Since then, an intermolecular sodium ion binding site has been identified to be common to isomorphous hirugen thrombin complexes crystallizing in space group C2 (unpublished results of this laboratory). Both RWJ-50353 and RWJ-50215 thrombin complexes crystallize in this space group, and each has two sodium ions with occupancies of about 0.85.

The final refinement reached convergence with an *R* value of 0.158 in the 7.0–2.3-Å resolution range, for the RWJ-50353 complex using 143 water molecules with an occupancy of >0.5 and $B < 45$ Å^2 ($\langle B \rangle = 28$ Å^2); the RWJ-50215 complex converged at an *R* value of 0.155 in the 7.0–1.8-Å resolution range, 161 water molecules with an occupancy of >0.5 and $B <$ 40 Å^2 ($\langle B \rangle = 26$ Å^2).

The omega angles of 97% of the peptide bonds of thrombin are within 6° of planarity, and the distribution of main-chain torsion angles of the complexes shows that all of the nonglycine amino acids fall within or close to the allowed regions in the Ramachandran map. The results from the final refinement cycles are listed in Table 1; they show that the deviations from ideal geometry are comparable for the two structures.

TABLE 1 Target values and deviations of refinement parameters from idealized geometry

		rms deviations	
	Target values	RWJ-50353	RWJ-50215
Distances			
Bond distance (Å)	0.015	0.015	0.016
Angle distance (Å)	0.030	0.044	0.042
Planar 1–4 distance (Å)	0.045	0.054	0.051
Miscellaneous			
Plane groups (Å)	0.030	0.030	0.032
Chiral centers (Å^3)	0.15	0.21	0.21
Nonbonded distances			
Single torsion (Å)	0.60	0.22	0.19
Multiple torsion (Å)	0.60	0.31	0.21
Possible X-Y H-bond (Å)	0.60	0.28	0.25
Torsion angles			
Planar (deg)	3	4	4
Staggered (deg)	15	20	20
Orthonormal (deg)	20	30	30
Thermal restraints			
Main-chain bond (Å^2)	1.0	1.1	1.1
Main-chain angle (Å^2)	1.5	1.9	1.8
Side-chain bond (Å^2)	2.0	2.6	2.8
Side-chain angle (Å^2)	2.5	3.8	4.1

RESULTS AND DISCUSSION

Thrombin

The thrombin structures of the two inhibitor complexes have an rms difference of 0.35 Å when their CA atoms are superposed. The thrombin structure (Fig. 1) shows no large differences from other isomorphous inhibitor complexes; the CA positions of the RWJ-50353 and RWJ-50215 structures have an rms difference of 0.19 Å and 0.32 Å compared to monoclinic PPACK-thrombin complex (Vijayalakshmi et al., 1994) and an rms difference of 0.33 Å and 0.22 Å compared to the DAPA complex, respectively (Mathews and Tulinsky, 1995).

Inhibitors

The active-site inhibitors have a well-defined electron density (Fig. 3). The binding of the inhibitors follows the two major modes of thrombin active site binding exemplified by the PPACK and argatroban/DAPA types, respectively. The PPACK class of inhibitors interact at the S2–S3 subsites with residues/groups that are in 2,3 positions of the inhibitor, whereas the argatroban class of inhibitors achieve similar interactions with their 1,3 residues. In both classes, the chain direction in the active site is antiparallel to the main-chain Ser214-Gly216 segment of thrombin, in contrast to the natural inhibitor hirudin, where a parallel β-strand is formed (Rydel et al., 1990, 1991; Grutter et al., 1990). Hirudin, however, exhibits the argatroban-like 1,3 binding mode through main-chain retro-binding (Tabernero et al., 1995).

Thiazole versus substrate-like binding at the S1′ subsite

The 2-benzothiazole in RWJ-50353 and 2-ketothiazole in RWJ-50215 bind at the S1′ subsite of thrombin. There they are surrounded by His57, Tyr60A, Trp60D ("backside"), and Lys60F, and, in the case of RWJ-50215, by the piperidine ring of the ligand (Fig. 4). This cavity, first inferred as the S1′ subsite from the position of the glycine linker of the divalent thrombin-hirulog 3 complex (Qiu et al., 1992), has subsequently been verified by the structures of similar complexes with hirutonin 2, hirutonin 6 (Zdanov et al., 1993), and CVS995 (Krishnan et al., 1996). Although the benzothiazole and thiazole rings bind to the S1′ subsite, their

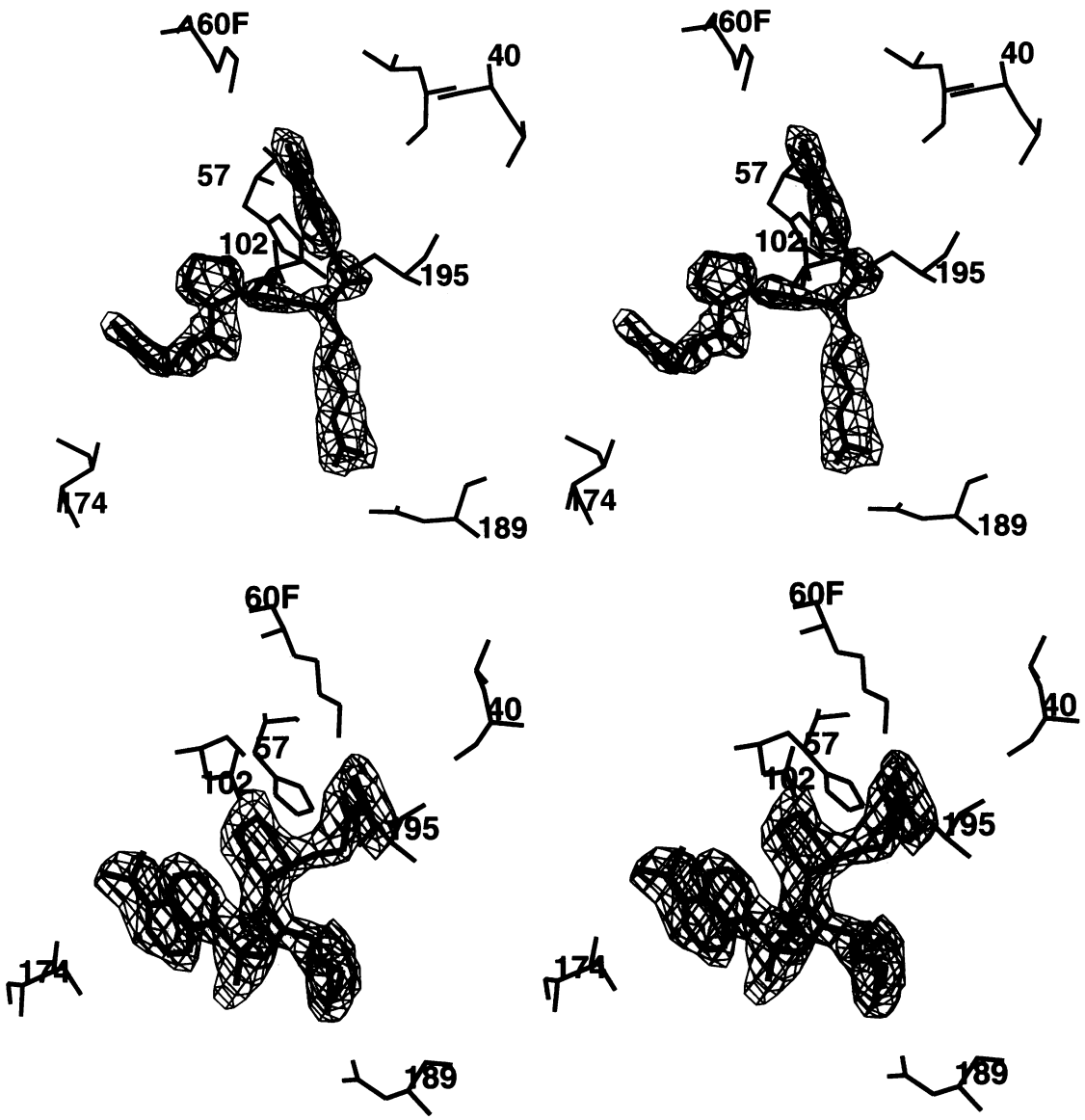

FIGURE 3 Stereo view of omit electron density of the RWJ inhibitors in their bound state. (*a*) RWJ-50353; (*b*) RWJ-50215. Basket contours at 1 sigma. Pertinent active site residues are as in Fig. 1.

interactions are significantly different because of their different size and shape.

The P1′ benzothiazole ring of RWJ-50353 has interactions with the catalytic His57 residue and with the Tyr60A-Thr60I insertion loop of thrombin. The N3 atom of the ring forms a direct hydrogen bond with His57NE2 (Table 2), and the indole ring of Trp60D stacks edge on to the benzothiazole ring (Fig. 4*a*). A similar hydrogen bond between His57NE2 and a nitrogen atom of a benzoxazole ring has been inferred in the crystal structure of a complex between porcine pancreatic elastase and Ac-Ala-Pro-Val-2-benzoxazole (Edwards et al., 1992). Although the oxygen and nitrogen positions could not be distinguished in the quasi-symmetrical benzoxazole ring, the nitrogen atom was positioned toward the His57, because the oxygen atom in the benzoxazole ring is a π-donor atom and is not expected to possess hydrogen bonding capability. Apart from stabilizing the overall structure in the active site, the hydrogen bond between the His57 and benzothiazole ring could aid in delocalizing the positive charge of a protonated His57 through the heterocyclic ring to the hemiketal oxygen atom, lending further stability to the transition state oxyanion. The sulfur atom points away from the active site and has a couple of close contacts with Glu192 (Table 2). The three terminal side-chain atoms of Lys60F move about 0.8 Å compared to Lys60F in the thrombin-hirugen complex to accommodate the bulky benzothiazole ring in the S1′ site (Fig. 5).

Both N3 and O of the 2-ketothiazole of the RWJ-50215 inhibitor form hydrogen bonds with the side chain of Lys60F (Figs. 4 *b* and 5). The latter is analogous to the hydrogen bond involving the carbonyl oxygen of a linker

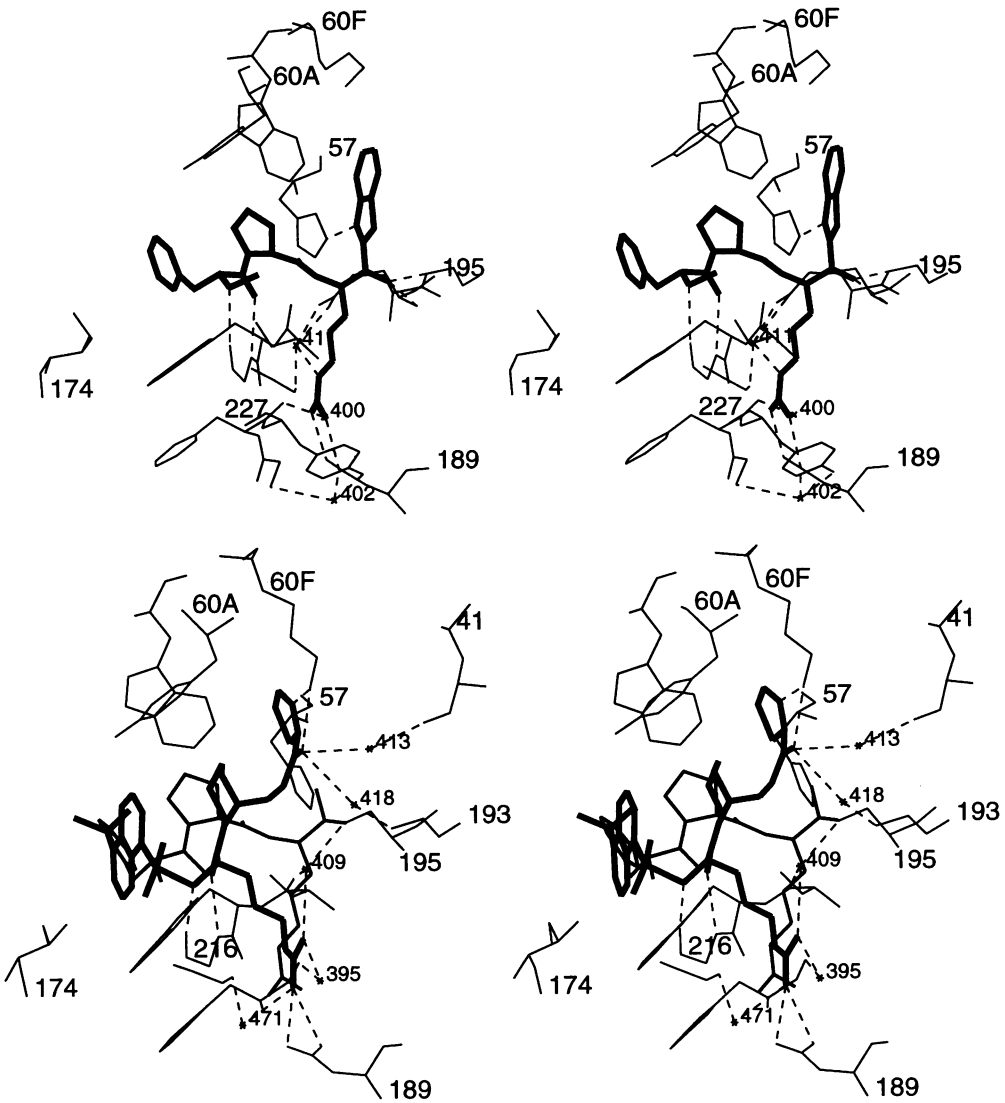

FIGURE 4 Stereo view of the binding of the RWJ inhibitors with thrombin. (a) RWJ-50353 in bold lines; thrombin in thin lines; hydrogen bonds in dotted thin lines; water positions in lowercase. (b) RWJ-50215 in bold lines; PPACK in medium; thrombin in thin; hydrogen bonds in dotted lines; water positions in lowercase.

glycine in the hirulog 3-thrombin structure (Qiu et al., 1992), although the oxygen positions are displaced by about 1.5 Å. The NZ of Lys60F also forms a hydrogen bond with His 57O, an interaction that is found in many other thrombin structures. Because the 2-ketothiazole is linked to the piperidine binding at S2, whereas the P1′ glycine residues of hirulog 3 and CVS995 are bonded to the P1 arginine, the pathways to the S1′ site are necessarily different (Fig. 5). After the Lys60F hydrogen bond, the thiazole ring forms a herringbone arrangement with Trp60D (Burley and Petsko, 1985), and the hirulog 3 chain goes off in a different direction. The carbonyl oxygen of RWJ-50215 is also linked to Leu41O and Gly193N through O_w413 and O_w418 (Fig. 4 *b*).

Natural thrombin substrates show a preference for residues with small side chains at the P1′ position. The preference of the S1′ subsite of thrombin for small P1′ residues, such as glycine or serine (Lottenberg et al., 1983) was postulated to be the result of the limited size of the subsite due to the protruding Lys60F residue (Qiu et al., 1992; Stubbs and Bode, 1993). This may be related to the observation that in the hirulog 3-thrombin structure, the P1′ glycine adopts a conformation that would be disallowed for any residue with a side chain. It seems, however, to be more than a simple fitting of a residue into the cavity, because the amino group of the Lys60F forms a hydrogen bond with the carbonyl oxygen atom of His57 in most cases, whether the S1′ subsite is unoccupied or occupied by a small residue like glycine in the hirulog 3-thrombin structure or the 2-ketothiazole ring in the RWJ-50215 structure. A bulkier group at the P1′ position, like the 2-benzothiazole in RWJ-50353, causes the Lys60F side chain to move away and disrupts the

TABLE 2 Interactions of the inhibitors in the active site of thrombin

Interactions		Distance (Å)	Type
RWJ-50353			
D-Phe	CZ-GLu97A 0	3.7	
D-Phe	CE1-Tyr60A OH	3.7	
D-Phe	CD2-Ile174 CD1	3.7	
D-Phe	CD2-Ile215 CE3	3.5	van der Waals
D-Phe	CD2-Ile215 CG	3.5	
D-Phe	CD2-Ile215 CB	3.6	
D-Phe	CD2-Ile215 CD2	3.6	
D-Phe	N-Gly216 O	2.9	H-bond
D-Phe	O-Gly216 N	3.0	H-bond
Pro	CB-His57 CD	3.9	
Pro	CB-Trp60D CH2	3.9	van der Waals
Pro	CG-Tyr60A CE2	3.9	
Arg	C-Ser195 OG	1.8	Transition state bond
Arg	NH1-Asp189 OD1	2.6	H-bonded ion pair
Arg	NH2-Asp189 OD2	2.7	H-bonded ion pair
Arg	O-Gly193 N	2.7	H-bond
Arg	O-Ser195 N	2.9	H-bond
Arg	NH1-Gly219 O	2.8	H-bond
Arg	NE-Ow411-Glu192 OE2	2.7,2.8	H-bonded solvent bridge
Arg	NH2-Ow400-Phe227 O	2.9,3.0	H-bonded solvent bridge
Arg	NH1-Ow411-Gly219 O	3.2,2.4	H-bonded solvent bridge
Ben	N3-His57 NE2	2.7	H-bond
Ben	S1-Glu192 CA	3.8	
Ben	S1-Glu192 CB	3.9	
Ben	S1-Gly193 N	3.4	
Ben	C4A-His57 CD2	3.8	
Ben	C4A-His57 NE2	3.7	
Ben	C7A-Trp60D CZ3	3.8	
Ben	C7-Trp60D CZ3	3.7	van der Waals
Ben	C6-Trp60D CZ3	3.7	
Ben	C6-Trp60D CE3	3.9	
Ben	C6-Lys60F NZ	3.5	
Ben	C5-Trp60D CZ3	3.8	
Ben	C4-His57 O	3.9	
Ben	C4-His57 CD2	3.6	
Ben	C4-His57 NE2	3.9	
RWJ-50215			
Dan	O1-Gly216 O	3.3	
Dan	S1-Gly216 O	3.6	
Dan	C2-Tyr60A OH	3.4	
Dan	C3-Tyr60A OH	3.3	
Dan	C2-Glu97A O	3.5	
Dan	C11-Leu99 CG	3.9	
Dan	C11-Leu99 CD2	3.6	van der Waals
Dan	C11-Leu99 CD1	3.4	
Dan	C7-Trp215 CE3	3.5	
Dan	C7-Trp215 CD2	3.9	
Dan	C8-Trp215 CZ3	3.9	
Dan	C8-Trp215 CE3	3.4	
Dan	C8-Gly216 C	3.5	
Dan	C8-Gly216 O	3.9	
Dan	C8-Glu217 CG	3.9	
Dan	C9-Gly216 C	3.8	
Dan	C9-Gly216 O	3.2	
Arg	O-Gly216 N	3.0	H-bond
Arg	N-Gly216 O	2.5	H-bond
Arg	NH1-Asp 189OD1	3.2	H-bonded ion pair
Arg	NH1-Asp 189OD2	2.9	H-bonded ion pair
Arg	NH2-Ow409O-Ser 195OG	3.2,2.7	H-bonded solvent bridge
	Ow409O-214O	2.7	H-bond
Arg	NH2-Ow395O-Phe 227O	3.2,2.9	H-bonded solvent bridge
Arg	NH1-Ow471O-Gly 219O	2.9,3.1	H-bonded solvent bridge
Pip	C2-Leu99 CB2	3.6	
Pip	C2-Trp215 CB	3.8	
Pip	C3-Leu99 CB2	3.5	
Pip	C3-Tyr60A CZ	3.9	
Pip	C3-Tyr60A CE1	3.9	
Pip	C4-Tyr60A (all atoms)	3.7–3.9	van der Waals
Pip	C4-His57 CD2	3.8	
Pip	C5-Trp60D CH2	3.5	
Pip	C5-Trp60D CZ3	3.6	
Tzl	S1-Trp60D CZ3	3.6	
Tzl	C4-Trp60D CZ3	3.1	
Tzl	C4-Trp60D CE3	3.6	
Tzl	N3-Lys60F NZ	3.0	H-bond
Tzl	O-Lys60F NZ	3.0	H-bond
Tzl	O-Ow413O-Leu41O	3.3,2.7	H-bonded solvent bridge
Tzl	O-Ow418O-Gly193N	3.5,2.8	H-bonded solvent bridge

hydrogen bond between His57 of the catalytic triad and Lys60F. That the interactions of Lys60F appear to play an important part in the biological activity of thrombin is in agreement with the mutation of Lys60F to glutamic acid, which leads to a significant reduction of clotting activity (Wu et al., 1991).

RWJ-50353 structure

As RWJ-50353 differs from PPACK only by the addition of a benzothiazole ring at the P1′ position, the overall interactions between thrombin and RWJ-50353 are similar to those in the thrombin-PPACK structure (rmsΔ = 0.52 Å). The inhibitor forms a hemiketal intermediate with the P1 arginine in the active site like PPACK. The carbonyl carbon atom has tetrahedral geometry in the complex (ArgC-Ser195OG 1.8 Å), with the carbonyl oxygen atom positioned in the oxyanion hole. The OG oxygen impinges nearly tetrahedrally on the carbonyl carbon atom of the arginine (CA-C-O = 109°, OG-C-O = 113°, OG-C-C2-Ben = 101°). The D-Phe-Pro-Arg motif has all of the interactions previously observed in inhibitor-thrombin complexes with this sequence binding in the active site (Table 2, Fig. 4 *a*): the doubly hydrogen-bonded ion pair of the P1 arginine guanidinum group with Asp189 in the S1 specificity pocket; the hydrophobic contacts with His57, Tyr60A, Trp60D, and Leu99 in S2 apolar site by Pro; and the formation of an antiparallel β-strand by the D-Phe-Pro-Arg sequence with the Ser214-Gly216 of thrombin (Bode et al.,

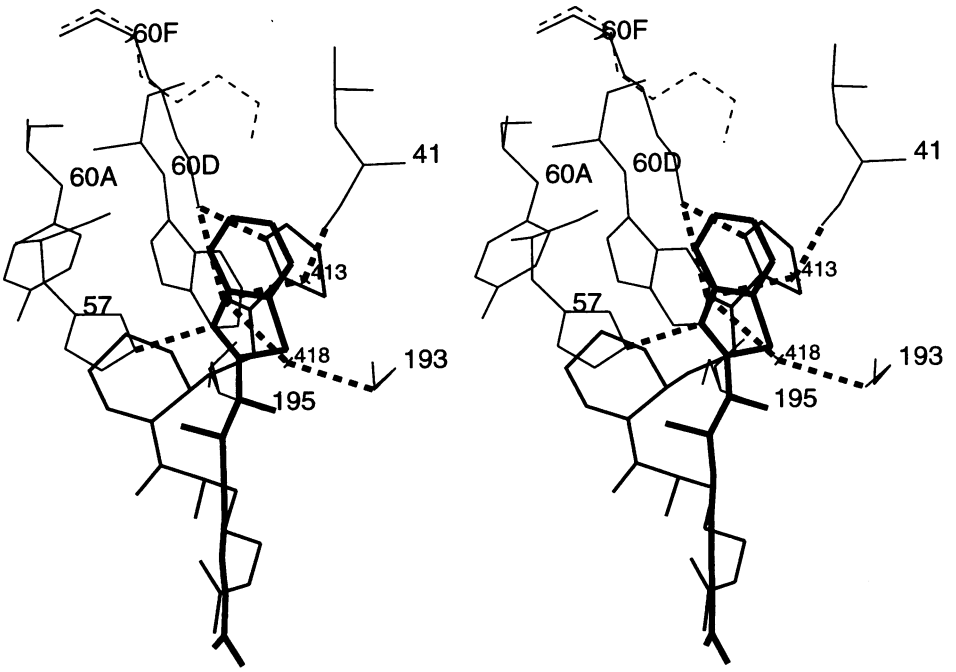

FIGURE 5 Stereo view of the S1′ binding site. RWJ-50353 in bold lines; RWJ-50215 in medium; thrombin in thin with Lys 60F of the RWJ-50353 structure in broken thin lines; hydrogen bonds in dotted bold lines.

1992). The water structure in and around the active site is conserved as in similar inhibitor-thrombin complexes (Krishnan et al., 1996). The Glu192 residue is ordered in the RWJ-50353–thrombin structure and interacts with arginine of the inhibitor through a water-mediated hydrogen bond (Glu192OE2-Ow411-ArgNE; Table 2).

RWJ-50215 structure

The interactions of RWJ-50215 with thrombin are similar to those of argatroban, NAPAP, 4-TAPAP (Banner and Hadvary, 1991; Brandstetter et al., 1992), and DAPA (Mathews and Tulinsky, 1995). Like argatroban and DAPA, it binds in a manner different from that of substrates, with CA of the P1 arginine displaced from that in PPACK-thrombin by 4.1 Å (Fig. 4 *b*). As a result, the arginine side chain forms a three-center hydrogen-bonded ion pair in the S1 site, in which NH1 interacts with both OD1 and OD2 of Asp189. Most of the other interactions in the argatroban and DAPA complexes are also retained in the present structure (Table 2): rms difference = 0.58 Å with 32 equivalent atoms in DAPA and 0.73 Å with 30 atoms in MQPA. The backbone N and O atoms of the P1 arginine hydrogen bond to Gly216 in an antiparallel manner.

Active-site water molecules mediate some additional thrombin-inhibitor interactions, where Ow409 bridges the NH2 group of arginine of the inhibitor with Ser195OG and Ser214O, and Ow395 connects the NH2 with Phe227O (Fig. 4 *b*). The oxygen atom of Gly219 interacts with the arginine side chain in two ways: by a hydrogen bond to the NE atom and indirectly to NH_2 through Ow471. A water molecule in the DAPA-thrombin structure bridged a sulfonyl oxygen of the dansyl group with Glu192 of thrombin. The presence of a water molecule at this site in the RWJ-50215 structure has not been confirmed.

The interactions of RWJ-50215 in the hydrophobic S2–S3 sites of thrombin (Fig. 4 *b*) are also similar to those of the argatroban structure. The dansyl group occupies the hydrophobic S3 site bounded by Trp60D and Ile174, and the naphthalene ring forms a herringbone pattern with Trp215 (Burley and Petsko, 1985) in a way analogous to that of the tetrahydroquinoline group of argatroban (Brandstetter et al., 1992). The piperidine ring adopts a chair conformation and binds at the S2 site surrounded by Leu99, His57, Tyr60A, and Trp60D. The electron density cannot distinguish between two opposite orientations of the dansyl dimethylamino substituent. Therefore, the methyl groups were oriented to maximize hydrophobic interactions with the naphthyl ring. The 4-ethylpiperidine group of DAPA makes that inhibitor stronger and more selective than related compounds (Okamoto et al., 1976). In RWJ-50215, the piperidine ring is substituted at the 2 position with an alkyl bridge to the ketothiazole group (Fig. 2) instead of a negatively charged 2-carboxylate group, as in argatroban or the 4-ethyl moiety of DAPA (Fig. 2). The electron density is consistent with the linker group in the axial position, which gives *R* stereochemistry at that carbon. The diastereomer with the opposite hand showed reduced biological activity (Bruce E. Maryanoff, private communication). The *R* configuration was also observed in the argatroban structure (Brandstetter et al., 1992).

The RWJ-50353 inhibitor binds much better to thrombin (K_i = 0.16 nM) than does RWJ-50215 (K_i = 1.2 μM). A number of factors contribute to the affinity of an inhibitor for an enzyme (Beveridge and DiCapua, 1989). The resemblance of RWJ-50353 to natural substrates probably ac-

counts for some of the difference. The highly electron-withdrawing benzothiazole group would be expected to increase the electrophilicity of the arginine carbon atom, leading to a stronger interaction with Ser195 OG (Costanzo et al., 1996). However, other factors must also be involved, because argatroban (Fig. 2), a molecule related to RWJ-50215, is an excellent inhibitor of bovine thrombin, with a K_i value of 14 nM (Kikumoto et al., 1984). Substituents on the piperidine ring of argatroban make hydrophobic interactions that are important in binding to the enzyme. A molecule similar to argatroban, except for a 4-methyl group on the piperidine ring, was a less potent inhibitor, with a K_i value of 310 nM. In contrast, removing only the 2-carboxylate group caused a much smaller K_i increase to 30 nM, whereas reversing the configuration at either carbon caused large decreases in inhibition. A similar trend was observed with DAPA (Kikumoto et al., 1980). A DAPA derivative without the 4-ethyl substituent gave a 10-fold higher IC_{50} value (1.0 versus 0.1 μM) in a clotting assay. Because the piperidine of RWJ-50215 occupies almost the same position as in DAPA and argatroban, substitution at the 4 position should lead to better inhibition. However, addition of the ketothiazole and the flexible alkyl linker may increase the entropy cost of binding RWJ-50215 to thrombin. Interest in such compounds related to DAPA and argatroban is driven by their nonpeptidic structures, by the much greater selectivity these molecules show for thrombin over trypsin, plasmin, and other proteases.

A survey of intramolecular arginine-carboxylate interactions in protein structures (Singh et al., 1987) indicates that the two specificity site arginine-aspartate geometries observed in the RWJ-50353 and RWJ-50215 complexes are not common. Twin N–twin O contacts, involving an arginyl NH1 and NH2 as found in RWJ-50353, occurred only once out of a total of 74 examples. Contacts involving NE and NH1 of the arginine were more common with 16 cases, and only four examples of three-center single N–twin O interactions were found like those in RWJ-50215. Single N–single O contacts were the most abundant, with 35 examples. It is difficult to reconcile the preference thrombin shows for the least likely salt bridge structures, unless it is related to the fact that its physiological specificity really arises from binding at the fibrinogen binding exosite.

We would like to thank Dr. John W. Fenton II for samples of human α-thrombin and the National Institutes of Health for grant HL25942 (AT).

REFERENCES

Ayala, Y., and E. DiCera. 1994. Molecular recognition by thrombin. Role of the slow→fast transition, site-specific ion binding energetics and thermodynamic mapping of structural components. *J. Mol. Biol.* 235: 733–746.

Banner, D., and P. Hadvary, 1991. Crystallographic analysis at 3.0-Å resolution of the binding to human thrombin of four active site-directed inhibitors. *J. Biol. Chem.* 266:20085–20093.

Beveridge, D., and F. DiCapua. 1989. Free energy via molecular simulation: applications to chemical and biomolecular systems. *Annu. Rev. Biophys. Biophys. Chem.* 18:431–492.

Blomback, B., M. Blomback, B. Hessel, and S. Iwanaga. 1967. Structure of N-terminal fragments of fibrinogen and specificity of thrombin. *Nature.* 215:1445–1448.

Bode, W., D. Turk, and A. Karshikov. 1992. The refined 1.9-Å X-ray crystal structure of D-Phe-Pro-Arg chloromethylketone-inhibited human alpha-thrombin: structure analysis, overall structure, electrostatic properties, detailed active-site geometry, and structure-function relationships. *Protein Sci.* 1:426–471.

Bode, W., D. Turk, and J. Sturzebecher. 1990. Geometry of binding of the benzamidine- and arginine-based inhibitors NAPAP and MQPA to human alpha-thrombin. X-ray crystallographic determination of the NAPAP-trypsin complex and modeling of NAPAP-thrombin and MQPA-thrombin. *Eur. J. Biochem.* 193:175–182.

Brandstetter, H., D. Turk, H. W. Hoeffken, D. Grosse, J. Sturzebecher, P. D. Martin, B. F. P. Edwards, and W. Bode. 1992. Refined 2.3 Å X-ray crystal structure of bovine thrombin complexes formed with the benzamidine- and arginine-based thrombin inhibitors NAPAP, 4-TAPAP, and MQPA: a starting point for improving antithrombotics. *J. Mol. Biol.* 226:1085–1099.

Burley, S. K., and G. A. Petsko, 1985. Aromatic-aromatic interaction: a mechanism of protein stabilization. *Science.* 229:23–28.

Costanzo, M. J., L. R. Hecker, M. R. Schott, S. C. Yabut, H. C. Zang, P. Andrade-Gordon, J. A. Kauffman, J. M. Lewis, R. Krishnan, A. Tulinsky, and B. E. Maryanoff. 1996. Potent thrombin inhibitors that probe the S1′ subsite. *J. Med. Chem.* 39:3039–3043.

Davie, E. W., K. Fujikawa, and W. Kisiel. 1991. The coagulation cascade: initiation, maintenance, and regulation. *Biochemistry.* 30:10363–10370.

DiCera, E., E. R. Guinto, A. Vindigni, Q. D. Dang, Y. M. Ayala, W. Meng, and A. Tulinsky. 1995. The Na^+ binding site of thrombin. *J. Biol. Chem.* 270:22089–22092.

DiMaio, J., B. Gibbs, Y. Konishi, J. Lefebre, and D. Munn. 1992. Synthesis of a homologous series of ketomethylene arginyl pseudodipeptides and applications to low molecular weight hirudin-like thrombin inhibitors. *J. Med. Chem.* 35:3331–3341.

Edwards, P. D., E. F. Meyer, Jr., J. Vijayalakshmi, P. A. Tuthill, D. A. Andisik, B. Gomes, and A. Strimpler. 1992. Design, synthesis, and kinetic evaluation of a unique class of elastase inhibitors, the peptidyl alpha-ketobenzoxazoles, and the X-ray crystal structure of the covalent complex between porcine pancreatic elastase and Ac-Ala-Pro-Val-2-benzoxazole. *J. Am. Chem. Soc.* 114:1854–1863.

Esmon, C. T. 1989. The roles of protein C and thrombomodulin in the regulation of blood coagulation. *J. Biol. Chem.* 264:4743–4746.

Esmon, N. L., W. G. Owen, and C. T. Esmon. 1982. Isolation of membrane-bound cofactor for thrombin-catalyzed activation of protein C. *J. Biol. Chem.* 257:859–864.

Finzel, B. C. 1987. Incorporation of fast Fourier transforms to speed restrained least-squares refinement of protein structures. *J. Appl. Crystallogr.* 20:53–55.

Grutter, M. G., J. P. Priestle, J. Rahuel, H. Grossenbacher, W. Bode, J. Hofsteenge, and S. R. Stone. 1990. Crystal structure of thrombin-hirudin complex: a novel mode of serine protease inhibitor. *EMBO J.* 9:2361–2365.

Hendrickson, W. A. 1985. Stereochemically restrained refinement of macromolecular structure. *Methods Enzymol.* 115:252–270.

Higashi, T. 1990. Auto-indexing of oscillation images. *J. Appl. Crystallogr.* 23:253–257.

Hijikata, A., S. Okamoto, E. Mori, K. Kinjo, R. Kikumoto, S. Tonomura, Y. Tamao, and H. Hara. 1976. In vitro and in vivo studies of a new series of synthetic thrombin-inhibitors (om-inhibitors). *Thromb. Res. Suppl. 2.* 8:83–89.

Hogg, D. H., and B. Blomback. 1978. The mechanism of the fibrinogen-thrombin reaction. *Thromb. Res.* 12:953–964.

Howard, A. J., G. L. Gilliland, B. C. Finzel, T. L. Poulos, D. H. Ohlendorf, and F. R. Salemme. 1987. The use of an imaging proportional counter in macromolecular crystallography. *J. Appl. Crystallogr.* 20:383–387.

Hung, D. T., T. K. H. Vu, V. I. Wheaton, K. Ishii, and S. R. Coughlin. 1992. Cloned platelet thrombin receptor is necessary for thrombin-induced platelet activation. *J. Clin. Invest.* 89:1350–1353.

Jackson, C. M., and Y. Nemerson. 1980. Blood coagulation. *Annu. Rev. Biochem.* 49:765–811.

Kikumoto, R., Y. Tamao, K. Ohkubo, T. Tezuka, and S. Tonomura. 1980. Thrombin inhibitors. 2. Amide derivatives of N-alpha-substituted L-arginine. *J. Med. Chem.* 23:830–836.

Kikumoto, R., Y. Tamao, T. Tezuka, S. Tonomura, H. Hara, K. Ninomiya, A. Hijikata, and S. Okamoto. 1984. Selective inhibition of thrombin by (2*R*, 4*R*)-4-methyl-1-[N^2-[(3-methyl-1,2,3,4-tetrahydro-8-quinolinyl) sulfonyl]-L-arginyl)]-2-piperidinecarboxylic acid. *Biochemistry.* 23: 85–90.

Krishnan, R., A. Tulinsky, G. P. Vlasuk, D. Pearson, P. Vallar, P. Bergum, T. K. Brunck, and W. C. Ripka. 1996. Synthesis, structure, and structure-activity relationships of divalent thrombin inhibitors containing an alpha-ketoamide transition state mimetic. *Protein Sci.* 5:422–433.

Lottenberg, R., J. A. Hall, M. Blinder, E. P. Binder, and C. M. Jackson. 1983. The action of thrombin on peptide *p*-nitroanilide substrates. Substrate selectivity and examination of hydrolysis under different reaction conditions. *Biochim. Biophys. Acta.* 742:539–557.

Marsh, H. C., Y. C. Meinwald, T. W. Thannhauser, and H. A. Scheraga. 1983. Mechanism of action of thrombin on fibrinogen. Kinetic evidence for involvement of aspartic acid at position P10. *Biochemistry.* 22: 4170–4174.

Mathews, I. I., K. P. Padmanabhan, V. Ganesh, A. Tulinsky, M. Ishii, J. Chen, C. W. Turck, S. R. Coughlin, and J. W. Fenton, II. 1994. Crystallographic structures of thrombin complexed with thrombin receptor peptides: existence of expected and novel binding modes. *Biochemistry.* 33:3266–3279.

Mathews, I. I., and A. Tulinsky. 1995. Active site mimetic inhibition of thrombin. *Acta Crystallogr.* D51:550–559.

Nesheim, M. E., F. G. Prendergast, and K. G. Mann. 1979. Interactions of a fluorescent active-site-directed inhibitor of thrombin: dansylarginine *N*-(3-ethyl-1,5-pentanediyl)amide. *Biochemistry.* 18:996–1003.

Okamoto, S., A. Hijikata, K. Ikezawa, K. Kinjo, R. Kikumoto, S. Tonomura, and Y. Tamao. 1976. A new series of synthetic thrombin-inhibitors (OM-inhibitors) having extremely potent and selective action. *Thromb. Res. Suppl. 2.* 8:77–82.

Qiu, X., K. P. Padmanabhan, V. E. Carperos, A. Tulinsky, T. Kline, J. M. Maraganore, and J. W. Fenton, II. 1992. Structure of the hirulog 3-thrombin complex and nature of the S′ subsites of substrates and inhibitors. *Biochemistry.* 31:11689–11697.

Rydel, T. J., K. G. Ravichandran, A. Tulinsky, W. Bode, R. Huber, C. Roitsch, and J. W. Fenton, II. 1990. The structure of a complex of recombinant hirudin and human alpha-thrombin. *Science.* 249:277–280.

Rydel, T. J., A. Tulinsky, W. Bode, and R. Huber. 1991. Refined structure of the hirudin-thrombin complex. *J. Mol. Biol.* 221:583–601.

Singh, J., J. M. Thornton, M. Snarey, and S. F. Campbell. 1987. The geometries of interacting arginine-carboxyls in proteins. *FEBS Lett.* 224:161–171.

Skrzypczak-Jankun, E., V. E. Carperos, K. G. Ravichandran, A. Tulinsky, M. Westbrook, and J. M. Maraganore. 1991. Structure of the hirugen and hirulog 1 complexes of alpha-thrombin. *J. Mol. Biol.* 221:1379–1393.

Stubbs, M. T., and W. Bode. 1993. A player of many parts: the spotlight falls on thrombin's structure. *Thromb. Res.* 69:1–58.

Tabernero, L., C. Y. Chang, S. L. Ohringer, W. F. Lau, E. J. Iwanowicz, W.-C. Han, T. C. Wang, S. M. Seiler, D. G. M. Roberts, and J. S. Sack. 1995. Structure of a retro-binding peptide inhibitor complexed with human alpha-thrombin. *J. Mol. Biol.* 246:14–20.

Tulinsky, A., and X. Qiu. 1993. Active site and exosite binding of alpha-thrombin. *Blood Coag. Fibrin.* 4:305–312.

Turk, D., J. Sturzebecher, and W. Bode. 1991. Geometry of binding of alpha-tosylated piperidines of *m*-amidino, *p*-amidino- and *p*-guanidino phenylalanine to thrombin and trypsin. X-ray crystal structures of their trypsin complexes and modeling of their thrombin complexes. *FEBS Lett.* 287:133–138.

Vijayalakshmi, J., K. P. Padmanabhan, K. G. Mann, and A. Tulinsky. 1994. The isomorphous structures of prethrombin2, hirugen-, and PPACK-thrombin: changes accompanying activation and exosite binding to thrombin. *Protein Sci.* 3:2254–2271.

Wu, Q., J. P. Sheehan, M. Tsiang, S. R. Lentz, J. J. Birktoft, and J. E. Sadler. 1991. Single amino acid substitutions dissociate fibrinogen-clotting and thrombomodulin-binding activities of human thrombin. *Proc. Natl. Acad. Sci. USA.* 88:6775–6779.

Zdanov, A., S. Wu, J. DiMaio, Y. Konishi, Y. Li, X. Wu, B. F. P. Edwards, P. D. Martin, and M. Cygler. 1993. Crystal structure of the complex of human alpha-thrombin and non-hydrolyzable bifunctional inhibitors, hirutonin-2 and hirutonin-6. *Proteins.* 17:252–265.